IRAQI BULLETIN OF GEOLOGY AND MINING (IBGM)\
IRAQ GEOLOGICAL SURVEY (GEOSURV-IRAQ)

*IBGM (**2025**, Vol 21; Issue 1)* *399-416*

GEOINFORMATICS-BASED AUTOMATED LANDFORM CLASSIFICATION AND ANALYSIS OF THEIR RELATIONSHIP WITH LANDSLIDE SUSCEPTIBILITY IN AKRE DISTRICT, KURDISTAN REGION, IRAQ

Kaiwan K. Fatah[1]* and Rebar T. Mzuri[1]

[1] Department of Earth Sciences and Petroleum, College of Science, Salahaddin University, Erbil, Kurdistan Region, Iraq; kaiwan.fatah@su.edu.krd; rebar.ali@su.edu.krd

***** *Corresponding author e-mail: kaiwan.fatah@su.edu.krd; Kaiwan K. Fatah (ORCID: 0000-0002-2535-8135)*

Type of the Paper (Article)
Received: 02/ 08/ 2024
Accepted: 18/ 03/ 2025
Available online: 27/ 06/ 2025

Abstract

Landforms are fundamental components of landscapes and pivotal elements within geomorphology. The comprehensive classification of landforms necessitates an advanced quantitative methodological approach capable of extracting discernible integral elements and patterns from Digital Elevation Models (DEMs). Identifying these patterns constitutes a crucial initial stage in recognizing and delineating landforms. The main objective of this research is to employ the Geomorphons technique at various scales, including neighborhood sizes of 5x5(3.9 km^2), 10x10(15.6 km^2), and 25x25(97.6 km^2) cells to autonomously categorize Geomorphic units (landforms) derived from 12.5-meter resolution ALOS PALSAR DEM within the SAGA-GIS software framework. Geomorphon is an effective model for characterizing the earth's morphology, encapsulating micro-landscape structures. Subsequently, the landform classes were correlated with landslide susceptibility zones through sophisticated spatial analysis functions in the designated area.

The study area was classified into 10 distinct types of the most prevalent geomorphic units, including flat, valley, slope, foot slope, peak, pit, ridge, hollow, shoulder, and spur. The results indicated that the predominant landform type observed is closely associated with slopes, while the least prevalent is flat terrain. Landform patterns exhibit a strong correlation with natural hazards, particularly landslides. Notably, approximately 100% of the flat regions are situated within low and very low landslide susceptibility zones, while more than 45% of the summit, ridge, shoulder, spur, and slope areas are characterized by high to very high landslide risk zones. The insights gained from this study are valuable for categorizing zones susceptible to landslide challenges. Understanding landforms is a critical parameter applicable to natural calamity assessment and future master planning in the Akre district of northern Iraq.

Keywords: Geomorphic Units; DEM; GIS and remote sensing techniques; Landslides vulnerability; Akre District.

ISSN 1811-4539, EISSN 3005-3714
https://doi.org/10.59150/ibgm2101a21
IBGM: http://ibgm-iq.org/
Academic Scientific Journals: www.iasj.net

1. Introduction

The Earth's surface is a mosaic of diverse landforms, formed by natural endogenic and exogenic processes (Robaina & Trentin, 2020; Stepinski & Jasiewicz, 2011; Zhazhlayi & Surdashy, 2022). Classifying terrain into landform types and segmenting specific terrains are crucial tasks across various scientific disciplines (Stepinski & Jasiewicz, 2011). These processes play a pivotal role in explaining the mechanisms underlying spatial heterogeneity in landscape evolution. Landforms provide physical boundaries for various mechanisms, including geology, ecosystem science, geomorphology, vegetation studies, hydrology, and archeology (Adeli et al., 2021). Landforms are spatial configurations of uniform surfaces formed by tectonic forces and surface processes (Alzekri et al., 2024; Seif, 2014). They are distinct geomorphic features on Earth's surface, spanning a wide range of spatial scales (Giano et al., 2020; Verhagen & Drăguţ, 2012). Identifying the components and patterns of landforms is crucial for comprehensive landscape analyses and environmental investigations (Adeli et al., 2021; Lin et al., 2021; Verhagen & Drăguţ, 2012; Yusra, 2019). Landform data analysis has multiple functions beyond geomorphological studies, providing information for landscape evaluation, process assessment, natural disaster prediction, and decision-making in regional planning, development, and management (Wahyuni et al., 2021).Various methodologies have been employed for collecting and analyzing such data, including visual interpretation techniques, quantitative analytical methods, statistical clustering, multivariate data analysis, filter methods, and geo-ecosystem modeling approaches (Adeli et al., 2021; Yusra, 2019). However, some approaches and models depend on classifying fundamental elements of the landscape. A method for detecting variations in landforms using remotely sensed data is substantial for identifying and classifying landscape features and landforms (Drăguţ & Eisank, 2012; Ngunjiri et al., 2020).

Geomorphometry is a novel discipline that uses statistical geomorphological characteristics to measure and analyze landforms. It is based on the association between roughness and quantitative factors (Adeli et al., 2021; Beranvand & Saife, 2020). Since the 1990s, automated landform classification has gained popularity due to the availability of accurate worldwide and national remotely sensed data (e.g., DEMs) and GIS techniques (Li et al., 2020; Robaina & Trentin, 2020). This method is more accurate, affordable, and time-effective than other techniques, establishing boundary criteria for various geomorphological phenomena (Ngunjiri et al., 2020; Stepinski & Jasiewicz, 2011). For example, Bety (2013) used DEMs to efficiently and effortlessly derive various topographic features, including three-dimensional representations, slope, aspect, and different types of convexities and curvatures. However, Morphometric parameters were previously calculated and analyzed manually, which was a laborious and expensive method (Shekar & Mathew, 2024). Numerous contemporary studies have employed automatic or semiautomatic algorithms to determine and classify landforms, with landforms being particularly significant from geological and engineering perspectives (Drăguţ & Eisank, 2012; Giano et al., 2020; Ilia et al., 2013; Lin et al., 2021; Robaina & Trentin, 2020). Al-Sababhah (2023) successfully classified the landforms of the Wadi Araba watershed in Jordan through the application of the Topographic Position Index (TPI), up to ten varied

landforms were found. Furthermore, the automated TPI technique based on geoinformatics was effectively utilized to categorize landforms in Zagros Mountain (Mokarram & Seif, 2014). The Geomorphon approach was applied to identify distinct landforms, contributing to terrain description, soil condition, and features assessment (Ngunjiri et al., 2020). Gioia et al. (2021) proposed that the Geomorphon technique is particularly effective and optimum for categorizing riverbed floor features. Additionally, Adeli et al. (2021) used the Geomorphon technique to classify landform units in the Arctic, which was considered particularly useful due to its capacity to discern distinct features that reflect regional processes and activities. In arid and semi-arid zones, the susceptibility to landslides is controlled by numerous spatial variables: topography, slope, elevation, LULC, watershed and drainage system characteristics, and patterns of precipitation duration and intensity (Fatah et al., 2024). Bachri et al. (2021) used geomorphometric parameters (stream networks, various indexes, and landform units), topographic factors (elevation, slope, and curvature), and environmental factors (LULC, NDVI, and rainfall data) as input variables in GIS platforms to identify potential landslide areas and risk level assessment for the eastern part of Indonesia, along with a study on the relationship of landslide susceptible zone and the causative factors with landform patterns.

This study aims to improve the accuracy of landform classification and mapping in the Akre district, northern Iraq. This region is prone to frequent mass movements, which pose risks to infrastructure, agriculture, and human settlements. Previous studies have largely relied on visual interpretation or traditional classification methods, limiting the precision of landform analysis in this region (Robaina et al., 2020; Bachri et al., 2021). Such approaches often fail to capture subtle topographic variations and spatial relationships between landform units, making them less effective for detailed geomorphological assessments. Thus, this study seeks to address this gap by utilizing the Geomorphon tool and using digital interpretation and spatial analysis techniques to evaluate the relationships between ten landform elements and landslide susceptibility zones. The aim is also to classify the terrain into essential geomorphological components for effortless analysis and interpretation. The Geomorphon method is chosen for its effectiveness in identifying landform units, allowing rapid visual analysis while preserving the intricacy of geomorphic patterns. This approach allows for vibrant differentiation between landform units within the study area. The findings will support landform mapping efforts, manage landslide susceptibility, and promote future urbanization in mountainous regions.

2. Materials and Methods

2.1. Description of the study area

Akre District area is located in the eastern portion of the Duhok Governorate, Kurdistan region. It is geographically positioned between longitude coordinates 43°30' – 44° 20'E and latitude coordinates 36°15' – 37°00'N. Covering an area of around (1832 Km²) with a height ranging from 310 and 1958 m above sea level according to the DEM (Figure 1). Iraq and the Kurdistan region, have a Mediterranean climate. Arid and semi-arid areas with two distinct seasons, a chilly, rainy winter (sometimes marked by floods) and a scorching, dry summer are its defining features (Fatah et al., 2022). The average yearly temperature is between 18 and 24 °C, while

the average yearly rainfall is between 450 and 1000 mm. The average monthly temperature is below freezing during the winter and can reach 48 °C during the summer (Fatah et al., 2020).

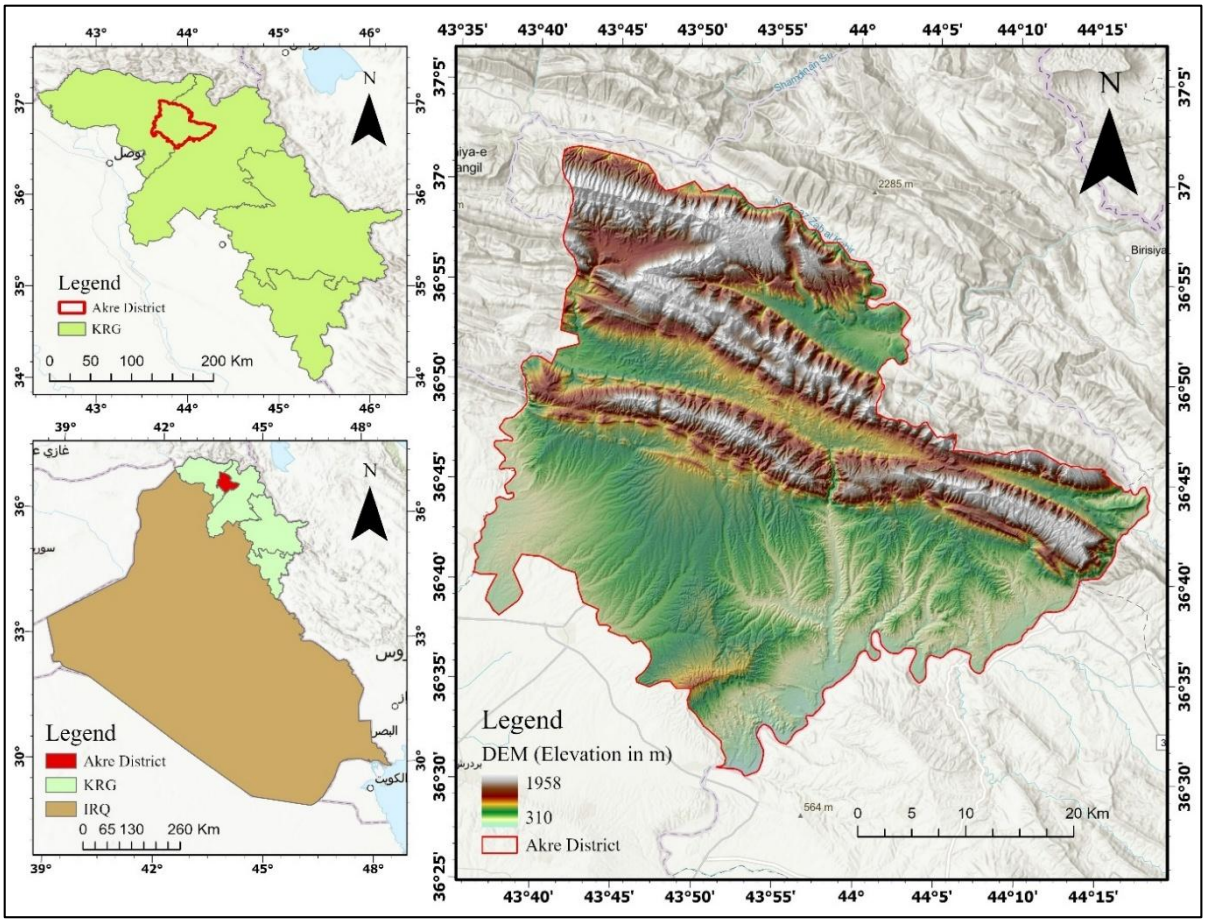

Figure 1. The location map of the study area.

According to the tectonic divisions of Iraq, the study area is located on the unstable shelf in the Low-Folded and High-Folded Zones (Fatah et al., 2024; Le Garzic et al., 2019). Numerous anticlines have been exposed in the area, including Bardarash and Sarta in the southern region and Peris, Akre, Perat, and Bijeel in the northern and northeastern regions (Fatah et al., 2022). The main geological formations exposed in the study area include Quaternary and recent sediments, along with the Bai-Hasan, Mukdadiya, Injana, and Fatha formations in the southern parts. Additionally, certain Cretaceous and Jurassic formations are present within the mountainous terrain in the northern parts (Figure 2; Fatah et al., 2024).

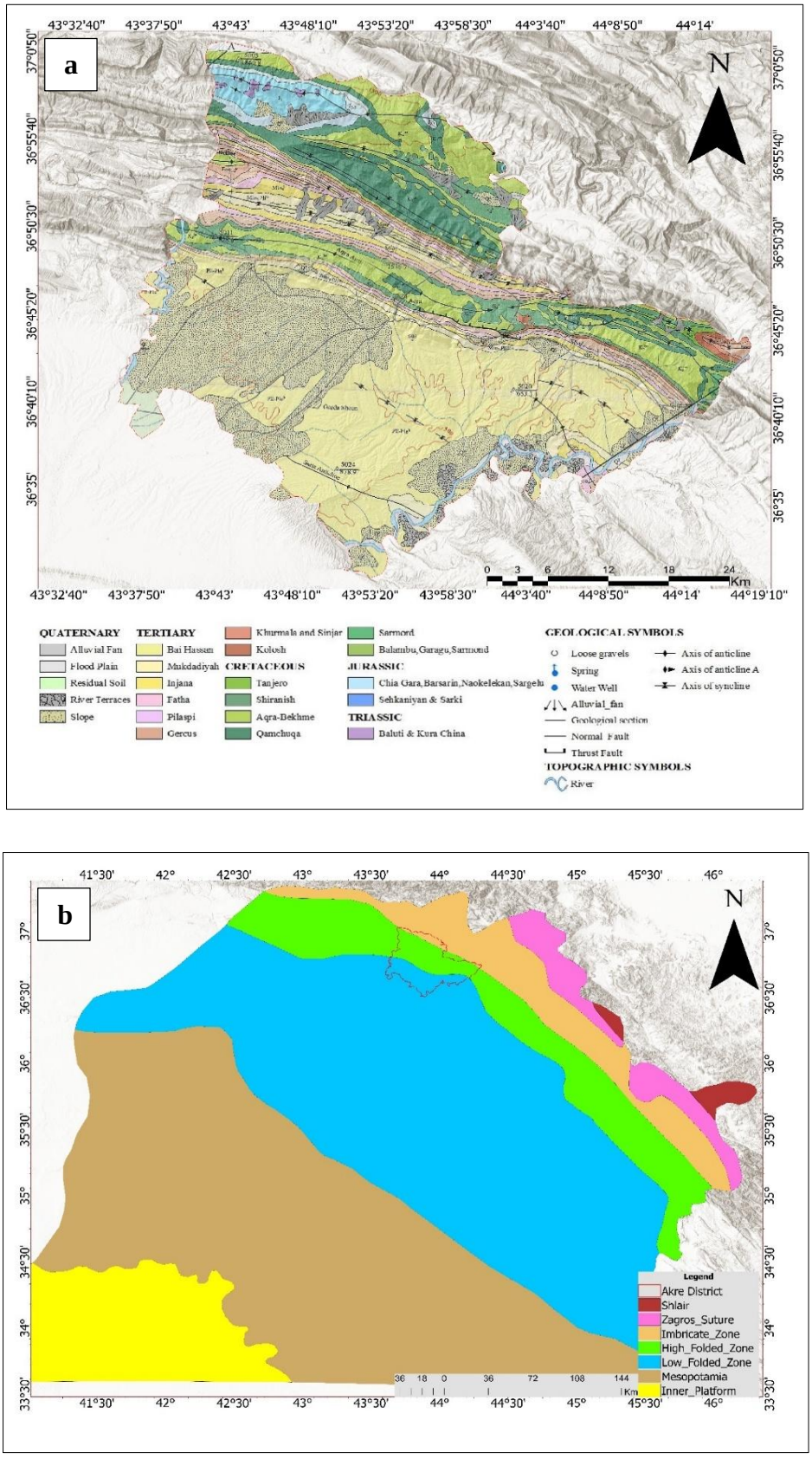

Figure 2. a) Geological map (Sissakian & Fouad, 2015) and b) the tectonic map of the study area after Fouad (2015).

2.2. Data acquisition and preprocessing

An Advanced Land Observing Satellite (ALOS) Phased Array type L-band Synthetic Aperture Radar (PALSAR) Digital Elevation Model (DEM) with 12.5 m spatial resolution for the area of interest was obtained from the Alaska Satellite Facility (2009) at https://search.asf.alaska.edu/#/. The DEM was subsequently subset to encompass the specific area of interest. Initially, the DEM data underwent pre-processing (filling sinks) to remove consecutive fill sinks and flat portions, ensuring accuracy and generating dependable results (Libohova et al., 2016). Furthermore, the Spatial Analyst tools, specifically the Fill tool, in the ArcGIS platform were employed to address and fill null pixels and remove missing values of altitude in the DEM (Fatah et al., 2024).

2.3. Methodology

The development of geospatial techniques and computer-based algorithms for evaluating geomorphometric characteristics of the topography of the Earth has promoted the growth of methods for semi-automated and automated recognition and categorization of landscape terrain regarding DEM data (Gioia et al., 2021). Consequently, the usefulness of landform classification based on map algebra has thus been documented in some studies that have been published (Libohova et al., 2016; Lin et al., 2021; Mihu-Pintilie & Nicu, 2019).

One of the most commonly employed methods for automatic landform classification in the SAGA-GIS software package is the Geomorphon. This study aims to classify landforms in the Akre district using the Geomorphon tool.

In this study, the landform classification methodology integrates the Geomorphon tool, an innovative technique introduced by Jasiewicz and Stepinski (2013). This technique marks a substantial advancement in the geomorphometry field, providing a robust, comprehensive, and adaptable framework for automated landform recognition and classification. The Geomorphon tool employs an advanced and sophisticated algorithm that merges altitude differentials with discernibility concepts to categorize topographic features into specific landform types. By leveraging the relationship between local topography and viewshed characteristics, this approach effectively infers the classification of landforms (Robaina et al., 2017). The present study performed geomorphon analysis utilizing ALOS PALSAR-DEM with 12.5 m resolution as input data in the SAGA GIS 7.8.1 and ArcGIS Pro.3.1 software platforms. This approach computes the elevation of a target pixel (central cell) in a DEM corresponding to its surrounding pixels in eight compass cardinal directions and up to a maximum search radius. It provides information about the type of landform at each central or target pixel position using a ternary pattern (Figure 3). It uses a ternary pattern to analyze the textural similarity of DEM with elevation fluctuations across adjacent cells at predefined scales (Adeli et al., 2021). The concept of this approach involves translating topographical data into a ternary pattern: elevations of neighboring pixels lower than the central cell are denoted as '-', equal elevations as '0', and higher elevations as '+' (Figure 3). This tripartite identification forms the basis for extracting

and identifying distinct types of landforms within the investigated region (Robaina & Trentin, 2020). This operator assigns an 8-tuple pattern to each central cell (focal pixel), applying a trinary scheme of symbols ('+', '0', or '-'). The pattern is generated by systematically comparing the central pixel (focal cell) with its eight surrounding cells (pixels), initiating the comparison from the easternmost pixel and proceeding counterclockwise direction. For instance, an 8-tuple pattern [-,+,-,+, -, 0, -, +] represents a specific configuration where the surrounding pixels are classified as (Adeli et al., 2021 higher, lower, equal, lower, higher higher, lower, equal, lower, higher) relative to the focal pixel.

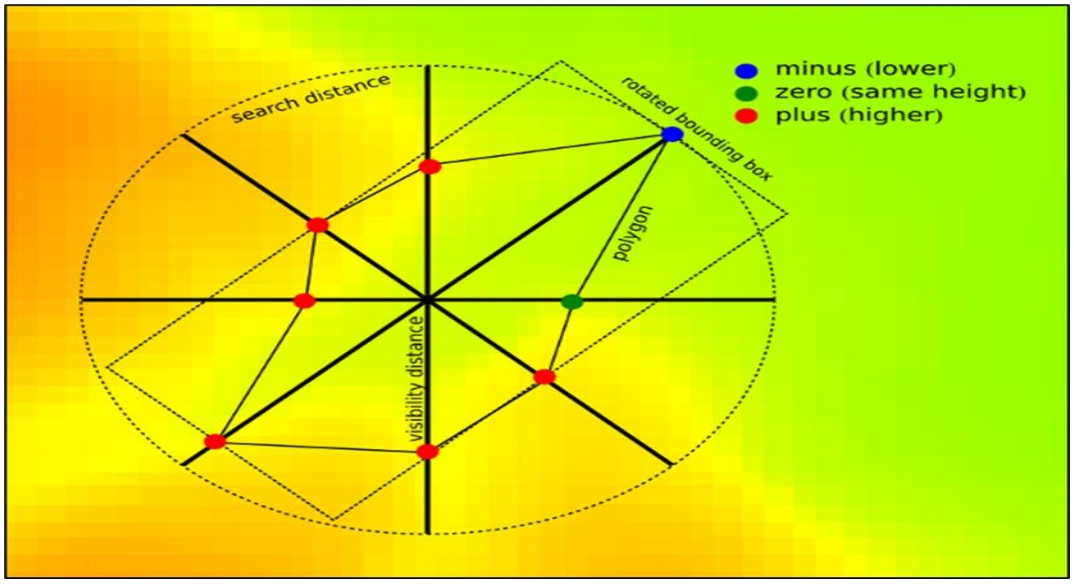

Figure 3. Application of the Ternary Local Patterns concept to the classification of landform components, as proposed by Jasiewicz and Stepinski (2013).

It is crucial to emphasize that the adjacent pixels in the grid configuration do not always align with the immediate proximity of the center pixel. They are calculated using the line-of-sight method across the eight cardinal directions, as explained by Stepinski and Jasiewicz (2011). Geomorphic classification is based on two main parameters: the relief threshold (D) and the search radius (L). The search radius specifies the greatest distance for determining zenith and nadir angles, whilst the relief threshold indicates the minimal divergence of these angles from the Earth's surface (horizontal plane). The Geomorphon tool was assessed across various configurations (scenarios), with the ideal values of 0.7 for the relief threshold and 5000 for the search radius chosen according to DEM resolution and terrain complexity, facilitating landform detection at a 12.5 m pixel resolution (Coria et al., 2024). This classification allocates values (‘+’, ‘0’, or ‘–’) to each cardinal direction (Figure 3) (Jasiewicz & Stepinski, 2013). The Geomorphon tool identifies 498 geomorphic patterns, which are further classified into 10 primary landform types—flat, pit, valley, foot-slope, hollow, slope, spur, shoulder, ridge, and peak—to meet research goals (Jasiewicz & Stepinski, 2013). This approach offers a comprehensive visualization of terrain morphology, including several topographic characteristics. Figure 4 illustrates a ternary local pattern, showcasing its application.

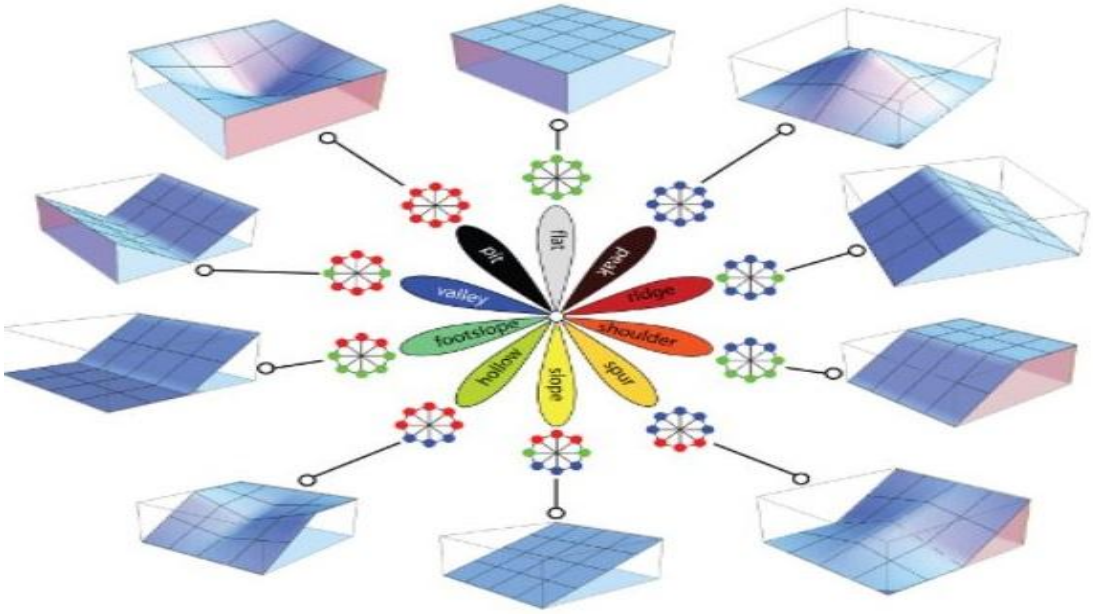

Figure 4. 3D symbolic visualizations and their representative geomorphons (ternary patterns) for the ten most prevalent landform types, as explained by Jasiewicz and Stepinski (2013).

Fatah et al. (2024) generated a landslide susceptibility map (LSM) for the Akre District using an ensemble method that incorporates the frequency ratio (FR) and analytic hierarchy process (AHP) models, based on geoinformatics techniques (Fatah et al., 2024). The generated LSMs have been classified into five classes depending on vulnerability levels: very high, high, moderate, low, and very low. The extrapolative effectiveness of the ensemble FR-AHP model was validated by employing the area under the curve of the receiver operating characteristic (AUC-ROC). The model attained an AUC-ROC value of 93.8%, indicating superior consistency and accuracy in LSM. This high-performance metric suggests that the ensemble F R-AHP method proposes an optimal methodology for evaluating landslide risk. Since this hybrid model was proved effective, this research adopted the base from LSM modeled by Fatah et al. (2024). That is because it would express landslide vulnerability in detail over the study area, hence improving possibilities of making informed decisions on land-use planning and risk management strategies.

Fatah et al. (2024) generated a landslide susceptibility map (LSM) for the Akre District using an ensemble method that incorporates the frequency ratio (FR) and analytic hierarchy process (AHP) models, based on geoinformatics techniques (Fatah et al., 2024). The generated LSMs have been classified into five classes depending on vulnerability levels: very high, high, moderate, low, and very low. The extrapolative effectiveness of the ensemble FR-AHP model was validated by employing the area under the curve of the receiver operating characteristic (AUC-ROC). The model attained an AUC-ROC value of 93.8%, indicating superior consistency and accuracy in LSM. This high-performance metric suggests that the ensemble FR-AHP method proposes an optimal methodology for evaluating landslide risk. Since this hybrid model was proved effective, this research adopted the base from LSM modeled by Fatah

et al. (2024). That is because it would express landslide vulnerability in detail over the study area, hence improving possibilities of making informed decisions on land-use planning and risk management strategies.

Geomorphic units were mapped with DEM data at three radii: 5, 10, and 25 cells based on the total number of pixels or cells in the circumference surrounding a targeted pixel to identify its Geomorphic Units (GU). Different window sizes were applied to geomorphic units to enhance the generalization and visualization of various landforms in this study. This approach allows for a more comprehensive representation of terrain features at multiple scales (Gioia et al., 2021). The LSM of the study area was overlaid with the geomorphic map, followed by the calculation of an area for every one of the ten most common geomorphic units falling into the landslide-susceptible zones on the LSM map. Visual interpretation and quantitative analysis with respect to field observation will be conducted in order to determine whether or not statistically significant relations exist between geomorphic units and landslide-susceptible zones. Furthermore, observation points, where morphological classification and assessment of landslide-prone zones were conducted, were marked on the Geomorphic maps that exhibited the strongest relationships with the landslide susceptible zones. This was performed to evaluate whether the landslide-prone areas identified at these points corresponded with the results obtained from the analysis of the LSM map in relation to Geomorphic units.

3. Results

The final geomorphon map (Figure 5) includes the ten most prevalent geomorphon types; flat, valley, slope, foot slope, peak, pit, ridge, hollow, shoulder, and spur. The Akre district's geomorphic patterns' geographic distribution is shown on the map.

Based on combined neighborhood sizes of 5*5, 10*10, and 25*25 cell sizes, landform classification was carried out. Such a combination can provide additional information about the general shape, and landforms of the area, and detailed information about the topography of the area under examination on larger scales. Figures 6 and 7 depict the ten generated landform classes, while Table 1 provides a description of the landform's areas for each cell size.

As a result, the various window sizes that were tested demonstrated how neighborhood size affected landform classifications, resulting in a variation in the landform area ratio between large and small values. For instance, the percentage area of the valley reduced from 9.47% to 7.66% and the percentage area of the slope decreased from 34.67% to 30.43% when the small cell size (5*5) was compared to the 10*10 cell size. The percentages for shoulder and spur increased from 6.71% to 8.42% and 13.86% to 18.29%, respectively (Table 1). However, during the comparison between cell size (5*5) and cell size (25*25), the percentage area of depression decreased from 2.71% to 1.97%, while the percentage of spur and hollow increased from 13.86% to 24.07% and 16.93% to 18.85 %, respectively (Table 1).

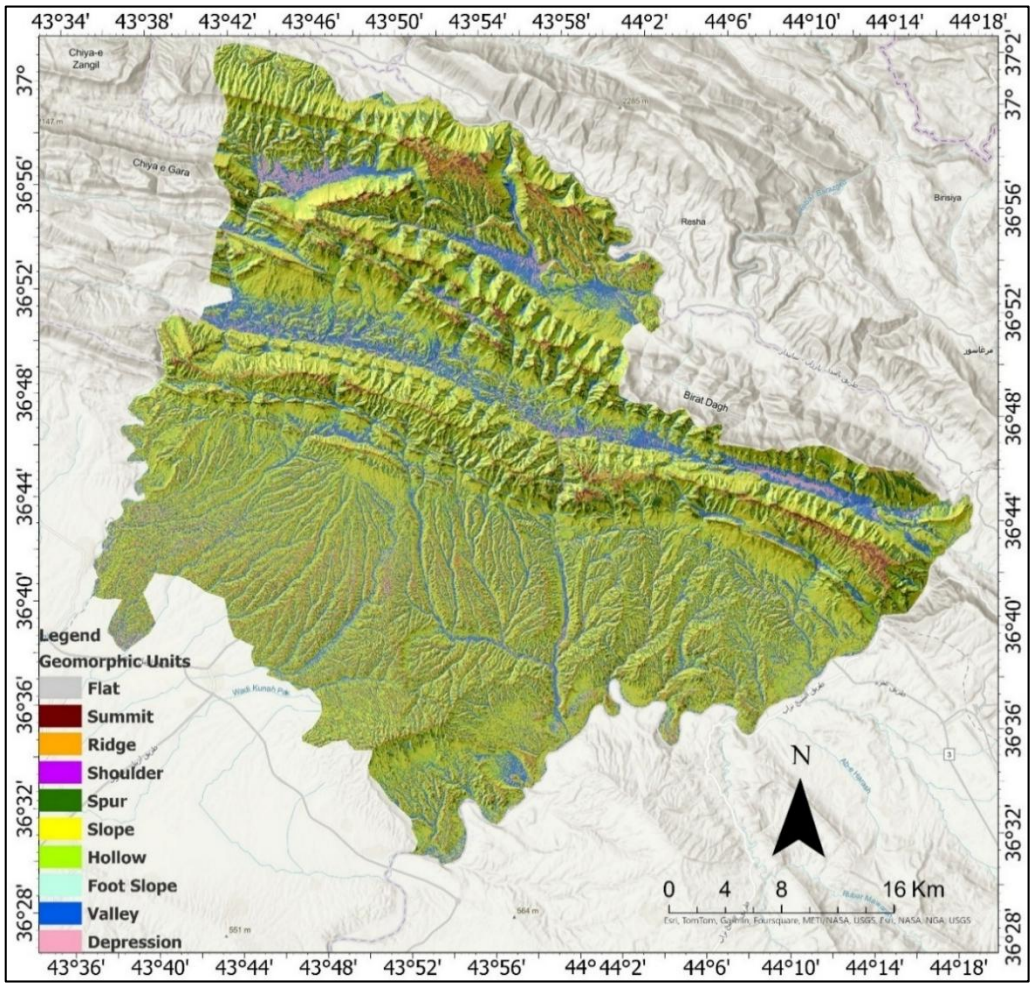

Figure 5. Geomorphon map of Akre district.

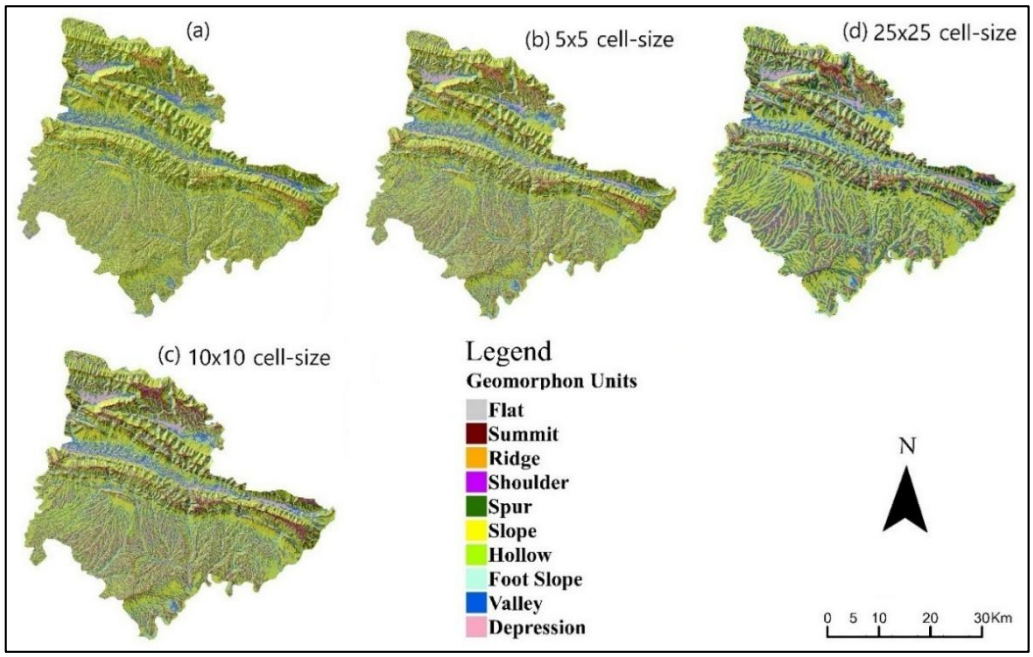

Figure 6. Landform classification based on different cell sizes.

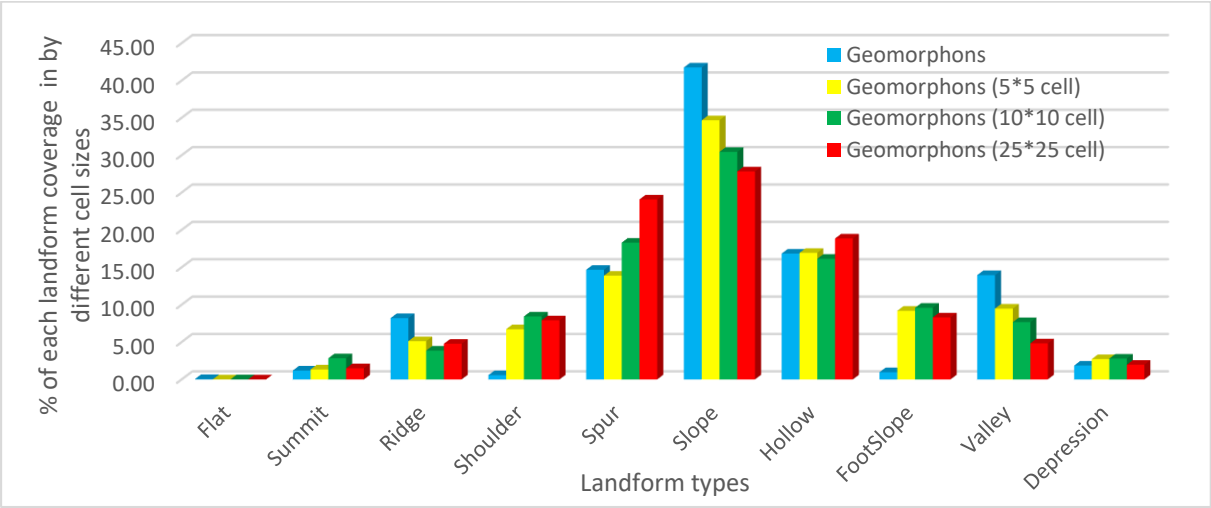

Figure 7. The area of landforms with different cell sizes.

Table 1. The distribution of different geomorphons cell size.

Landforms based on Geomorphons	Geomorphons		Geomorphons (5*5 cell)		Geomorphons (10*10 cell)		Geomorphons (25*25 cell)	
	Area (km²)	%	Area (km²)	%	Area (km²)	%	Area (km²)	%
Flat	0.86	0.05	0.08	0.01	0.31	0.02	0.09	0.01
Summit	21.69	1.18	24.42	1.33	51.80	2.83	27.29	1.48
Ridge	150.23	8.20	93.71	5.11	70.51	3.85	87.52	4.78
Shoulder	10.42	0.57	122.90	6.71	154.29	8.42	144.78	7.90
Spur	268.62	14.66	254.19	13.86	335.14	18.29	440.91	24.07
Slope	764.72	41.74	635.24	34.67	557.57	30.43	509.70	27.82
Hollow	308.42	16.83	310.17	16.93	295.58	16.13	345.43	18.85
Foot Slope	17.60	0.96	168.18	9.18	175.52	9.58	151.96	8.29
Valley	255.54	13.95	173.48	9.47	140.34	7.66	88.40	4.82
Depression	33.99	1.86	49.73	2.71	51.02	2.79	36.01	1.97
Total	1832.08	100	1832.08	100	1832.08	100	1832.08	100

The landslide susceptibility map generated from a previous study has been used to correlate the spatial distribution of the geomorphic types within the studied area. The landslide map is classified into five classes: very high, high, moderate, low, and very low (Figure 8), while Table 2 shows the percentage of each class.

Table 2. The percentage area of landslide-prone zones.

Landslide Prone Zones	Area (km²)	Percentage (%)
Very low	164.6	9.0
Low	449.1	24.5
Moderate	473.7	25.9
High	462.4	25.2
Very high	282.2	15.4
Total	1832.0	100.0

The results in Table 3 indicate that more than 45% of the areas of summit, ridge, shoulder, spur, and slope, are classified as having high to very high landslides; these regions can be found in the north, east, and west of the study area and the anticline that extends from east to west of the Akre district. These areas are highly vegetated, with relief between 900 – 1500 m, bedrock mainly consisting of limestone and dolomitic limestone, well-drained soil, and limited human activity.

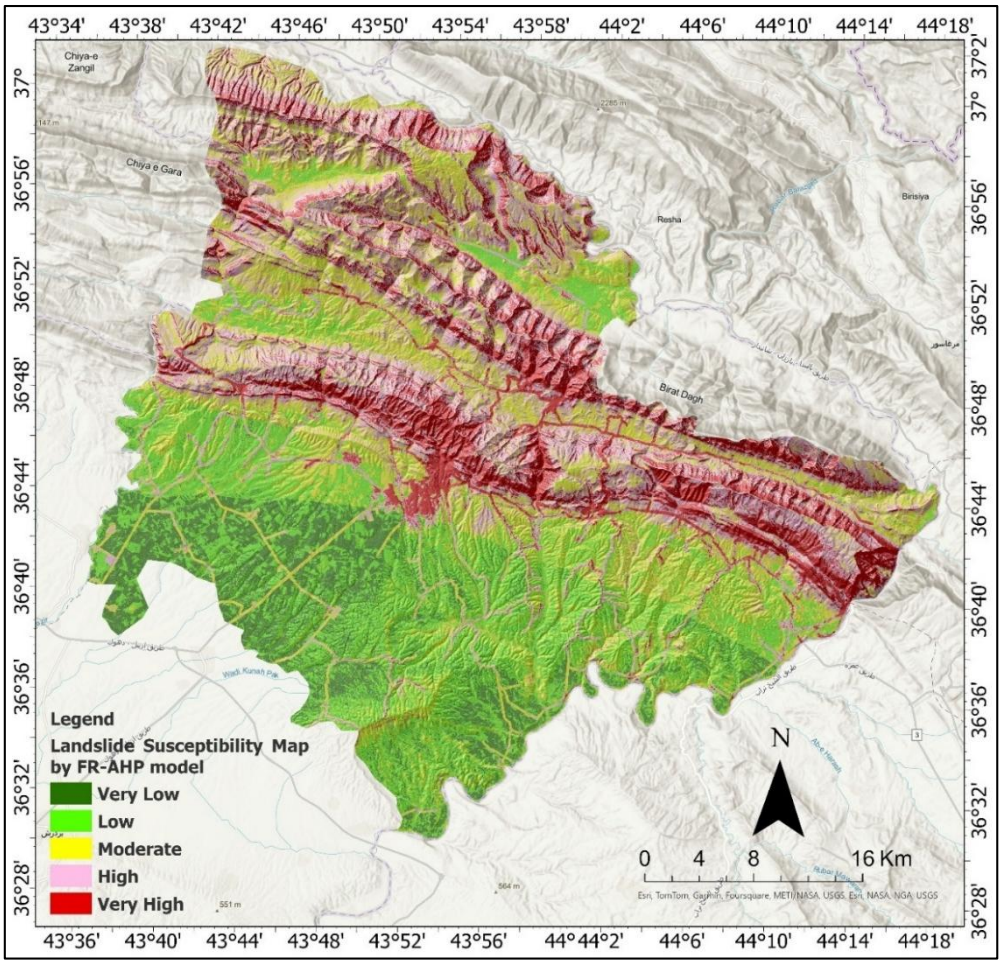

Figure 8. Landslide susceptibility map of Akre district (modified after Fatah et al., 2024).

Moreover, the hollow, foot slope, valley, and depression are classified as having moderate to high landslides with percentages of 62.82%, 67.8%, 71.25%, and 62.33% respectively; these areas are located in the central parts of the studied area, northern, and western (Figure 8). These areas are elevated between 750 and 900 m covered by siltstone, sandstone, and marly limestone, and limited human activities (Figures 1 and 2).

Finally, the results show that 69.23% and 30.77% of the flat units are classified as very low and low landslides respectively, which cover the southern part of the area; these areas are characterized by less vegetative coverage and limited rainfall (Table 3). Lithologically, the area is composed of recent deposits and mudstone, relief less than 600 m, and highly affected by human activities.

Table 3: The landforms area for each landslide-prone zone.

Landforms	Very Low	Low	Moderate	High	Very High	Total
Flat	69.23	30.77	0.00	0.00	0.00	100
Summit	0.19	3.58	49.94	43.04	3.26	100
Ridge	4.14	10.39	28.09	41.49	15.88	100
Shoulder	10.12	23.34	18.90	27.43	20.22	100
Spur	9.79	24.95	20.28	25.69	19.29	100
Slope	9.63	26.30	24.70	23.96	15.41	100
Hollow	10.01	27.16	27.78	21.95	13.10	100
FootSlope	8.10	24.10	33.28	24.37	10.15	100
Valley	3.07	25.68	45.24	19.44	6.57	100
Depression	0.27	37.40	43.43	11.73	7.16	100

The Akre district experiences landslide processes due to fluctuations in slope degree, unpredictable or low amounts of rainfall, human activities, and varying lithology. Due to erratic or infrequent rainfall, the area frequently experiences droughts and the resulting vegetation degradation, which exacerbates the landslide processes in the area. Figure 9 displays field images of landslide incidents that have occurred in the Akre District. This figure illustrates high-risk sites that have steep slopes and diverse lithology. A landslide susceptibility map is shown in the center of the figure, while field photographs depict a variety of different types of landslides (mass wasting, debris, and rock fall). The danger is increased in areas with steep terrain and construction sites for roads. It is essential to implement mitigation strategies such as slope stabilization and appropriate drainage systems in order to minimize the likelihood of landslides occurring in the area.

Figure 9: Landslide susceptibility map and Landslide incidents field photos units of Akre district with filed photos.

To validate the final map, from each class of Landslide a specific area was selected to correlate with the spatial distribution of geomorphic types in the area. Site 1 represents very high to high susceptible areas to landslide, site 2 shows high landslide, site 3 indicates moderate landslide, and low to very low is present at site 4. Based on field observations and high-resolution Google Earth, these places were selected for visual validation. The findings demonstrated a high degree of agreement between the field observation landform survey, Google Earth photos, and the final landslide map (Figure 10).

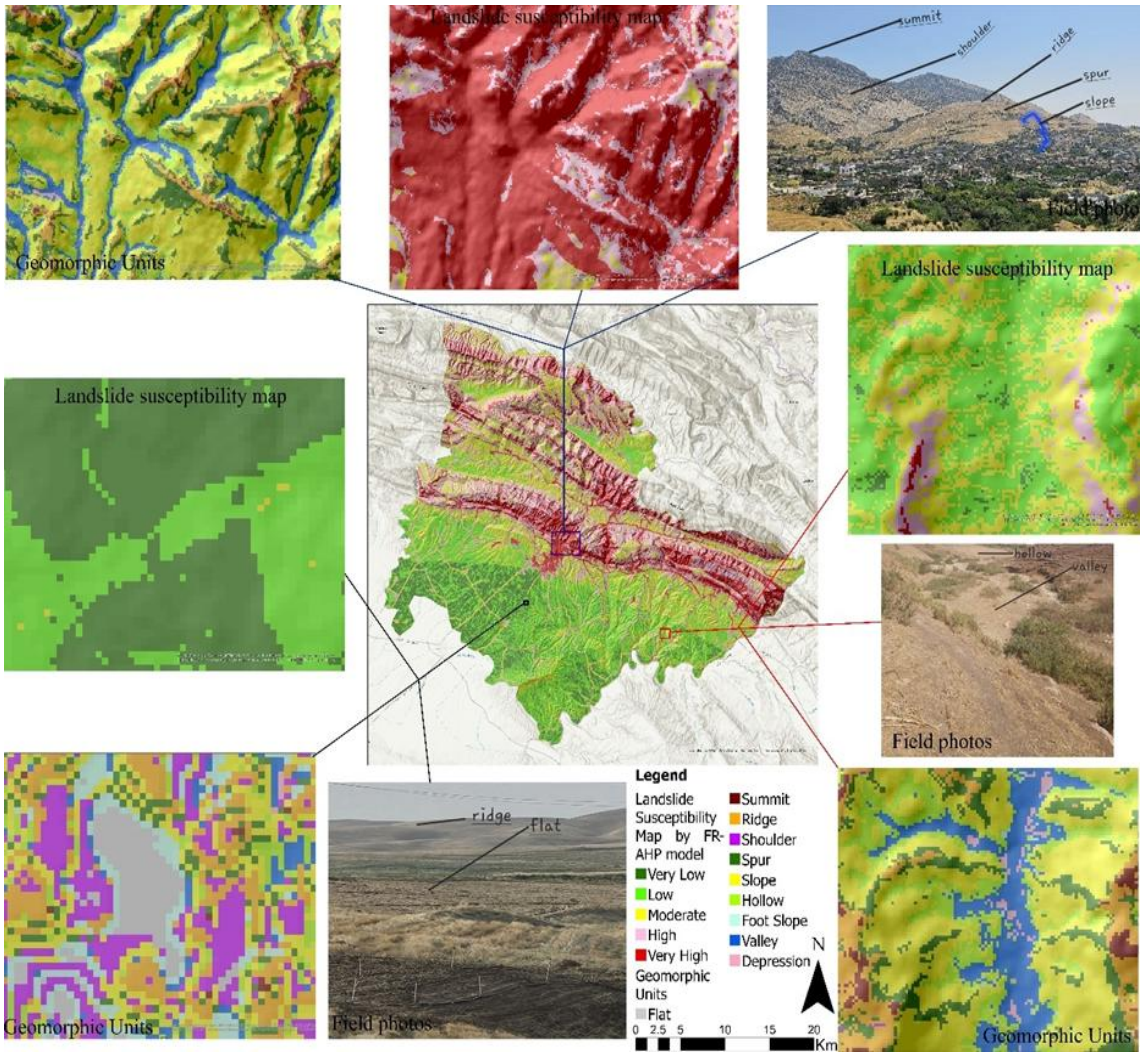

Figure 10: Visual validation of Landslide susceptibility map and Geomorphic units of Akre district with filed photos.

The automatic classification of landforms with computer-based models is a considerably more accurate, cost-effective, and productive approach to categorizing the landforms on the surface of the Earth. This classification establishes boundary conditions for several geomorphological phenomena (Libohova et al., 2016). The most common landform form found is strongly correlated with slope, whilst the least common is correlated with flat terrain. These conclusions were reached by comparing the results of the identification and extraction processes with field

observations. The findings of the research clarified the surface morphologies and underlying mechanisms that have formed and are shaping this region's terrain. It is evident that the evolution of topographic features such as shoulders, spurs, and hollows has progressed further in the ridge and valley regions. Ultimately, the extracted model facilitated the identification of landform elements and patterns of topographic variation, which in turn highlighted disparities, resemblances, and instabilities in terrain morphology (Alzekri et al., 2024; Fatah et al., 2024).

Five classifications were identified on the final Landslide map. According to Table 2, these classifications are very low, low, moderate, high, and very low. The low and very low areas are primarily in the south of the Akre district and are primarily covered by recent deposits, according to the spatial distribution of landslides (Figure 8). It is evident that there are numerous moderate landslide zones in the northern and central regions of the study area which were characterized by slope, spur, and shoulder landforms. Finally, high and very high classes are in the northern, some central, and northwest regions of the Akre district; these areas are primarily mountainous areas that have been affected by human activity and have scant vegetation. In summary, the studied area's landslides are predominantly distributed in the northern directions. However, the study area's center parts also have a high rate of landslides, primarily as a result of the topography of the area and human activity. The results of the present study are parallel with previous studies (Adeli et al., 2021; Beranvand & Saife, 2020).

The resolution of the DEM data is one of the method's limitations when it involves employing a digital elevation model to map landforms. The accuracy in determining particular landforms, particularly smaller or more complex ones, can be affected by the detailed resolution of the topographical model. More comprehensive maps can be produced with higher-resolution data, however, there may be additional processing expenses and requirements. The possibility of inaccuracies and errors in the elevation data is another drawback of landform mapping by digital elevation model, which requires preprocessing. The overall accuracy and quality of the mapped features might be negatively impacted by inaccurate depictions of landforms resulting from inaccurate elevation measurements. Thus, since mapping landforms using DEM, it's critical to take accuracy and data sources into account. Nevertheless, this technique uses an 8-tuple pattern of the visible neighborhood, which circumvents the commonly encountered drawback of conventional calculus techniques, which are unable to identify all terrain forms within a single window size (Ngunjiri et al., 2020).

The Geomorphon technique has been widely used for landform mapping (Jasiewicz & Stepinski, 2013; Libohova et al., 2016; Robaina & Trentin, 2020) and is employed in this study to identify and classify landforms based on their geomorphologic appearances and spatial distribution. The findings contribute to a more comprehensive understanding of landform patterns and their classification.

6. Conclusions

The Geomorphon approach has been effectively implemented to locate and recognize landform features in the Akre district. The findings of this research were juxtaposed with a landslide

susceptibility map to determine the geographical distribution of landforms in the studied area. The study's findings indicated the surface shapes and types of processes that have or are currently operating in the region. The results revealed that slopes account for the maximum percentage of the research area, while flats (plains) represent the smallest percentage. Furthermore, it has been demonstrated that the slope, hollow, and spur landforms collectively constitute the dominating landform patterns, accounting for around three-quarters of all categories under the tenth Geomorphon units. Hence, the landslide has happened in the shoulder, spur, slope, hollow, and foot slope elements, and a very high landslide has occurred in the ridge and summit. This study demonstrates that the created model is a useful tool for analyzing the spatial distribution of geomorphon types and landslides that can qualitatively analyze landslides over a sizable territory by combining remotely sensed data with GIS approaches.

References

Adeli, Z., Ghahroudi Tali, M., & Sadough, H. (2021). Application of Geomorphons method in identifying landform elements (Case study: Hablehroud Basin) *Quantitative Geomorphological Research*, *10*(2), 106-119. https://doi.org/10.22034/gmpj.2021.255287.1222

Al-Sababhah, N. (2023). Topographic position index to landform classification and spatial planning, using GIS, for Wadi Araba, South West Jordan. *Environment Ecology Research*, *11*(1), 79-101. https://doi.org/DOI: 10.13189/eer.2023.110106

Alzekri, O. A., Al-Ali, A. K., & Soltan, B. H. (2024). Neotectonics for the Rumaila Oilfield, Southern Iraq, Using InSAR Techniques. *Iraqi Geological Journal*, *57*(1C), 146-164. https://doi.org/https://doi.org/10.46717/igj.57.1C.11ms-2024-3-23

Bachri, S., Shrestha, R. P., Yulianto, F., Sumarmi, S., Utomo, K. S. B., & Aldianto, Y. E. (2021). Mapping Landform and Landslide Susceptibility Using Remote Sensing, GIS and Field Observation in the Southern Cross Road, Malang Regency, East Java, Indonesia. *Geosciences*, *11*(1), 4. https://doi.org/https://doi.org/10.3390/geosciences11010004

Beranvand, H., & Saife, A. (2020). Identification, classification and morphometry of glacial cirque in Jupar altitude of Kerman %J Quantitative Geomorphological Research. *8*(4), 63-80. https://doi.org/10.22034/gmpj.2020.106412

Bety, A. K. (2013). Urban geomorphology of Sulaimani City, using remote sensing and GIS techniques, Kurdistan Region, Iraq. *Unpublished PhD thesis, Faculty of Science and Science Education, University of Sulaimani*, 125.

Coria, R. D., Brungard, C., Vizgarra, A. L., Moretti, L. M., Schulz, G. A., & Rodríguez, D. M. (2024). Accuracy assessment of the geomorphon approach to detect ecological sites in the Dry Chaco region of Argentina. *Catena*, *246*, 108409.

Drăguţ, L., & Eisank, C. (2012). Automated classification of topography from SRTM data using object-based image analysis. *Geomorphometry*, 141-142.

Fatah, K. K., Hamed, M., Saeed, M. H., & Dara, R. (2020). Evaluation groundwater quality by using GIS and water quality index techniques for wells in Bardarash area, Northern Iraq. *The Iraqi Geological Journal*, *57*(2C), 87-104.

Fatah, K. K., Mustafa, Y. T., & Hassan, I. O. (2022). Flood Susceptibility Mapping Using an Analytic Hierarchy Process Model Based on Remote Sensing and GIS Approaches in Akre District, Kurdistan Region, Iraq. *Iraqi Geological Journal*, *55*(2C), 121-149. https://doi.org/10.46717/igj.55.2C.10ms-2022-08-23

Fatah, K. K., Mustafa, Y. T., & Hassan, I. O. (2024). Geoinformatics-based frequency ratio, analytic hierarchy process and hybrid models for landslide susceptibility zonation in Kurdistan Region, Northern Iraq. *Environment, Development and Sustainability*, *26*(3), 6977-7014. https://doi.org/10.1007/s10668-023-02995-7

Fouad, S. F. (2015). Tectonic map of Iraq, scale 1: 1000 000, 2012. *Iraqi Bulletin of Geology and Mining*, *11*(1), 1-7.

Giano, S. I., Danese, M., Gioia, D., Pescatore, E., Siervo, V., & Bentivenga, M. (2020). Tools for semi-automated landform classification: a comparison in the Basilicata Region (Southern Italy). International Conference on Computational Science and Its Applications,

Gioia, D., Danese, M., Corrado, G., Di Leo, P., Minervino Amodio, A., & Schiattarella, M. (2021). Assessing the Prediction Accuracy of Geomorphon-Based Automated Landform Classification: An Example from the Ionian Coastal Belt of Southern Italy. *ISPRS International Journal of Geo-Information*, *10*(11). https://doi.org/10.3390/ijgi10110725

Ilia, I., Rozos, D., & Koumantakis, I. (2013). Landform classification using GIS techniques. The case of Kimi municipality area, Euboea island, Greece. *Bulletin of the Geological Society of Greece*, *47*(1), 264-274.

Jasiewicz, J., & Stepinski, T. F. (2013). Geomorphons — a pattern recognition approach to classification and mapping of landforms. *Geomorphology*, *182*, 147-156. https://doi.org/https://doi.org/10.1016/j.geomorph.2012.11.005

Le Garzic, E., Vergés, J., Sapin, F., Saura, E., Meresse, F., & Ringenbach, J. (2019). Evolution of the NW Zagros Fold-and-Thrust Belt in Kurdistan Region of Iraq from balanced and restored crustal-scale sections and forward modeling. *Journal of Structural Geology*, *124*, 51-69. https://doi.org/10.1016/j.jsg.2019.04.006

Li, S., Xiong, L., Tang, G., & Strobl, J. (2020). Deep learning-based approach for landform classification from integrated data sources of digital elevation model and imagery. *Geomorphology*, *354*, 107045. https://doi.org/https://doi.org/10.1016/j.geomorph.2020.107045

Libohova, Z., Winzeler, H. E., Lee, B., Schoeneberger, P. J., Datta, J., & Owens, P. R. (2016). Geomorphons: Landform and property predictions in a glacial moraine in Indiana landscapes. *CATENA*, *142*, 66-76. https://doi.org/10.1016/j.catena.2016.01.002

Lin, S., Chen, N., & He, Z. (2021). Automatic Landform Recognition from the Perspective of Watershed Spatial Structure Based on Digital Elevation Models. *Remote Sensing*, *13*(19), 3926. https://www.mdpi.com/2072-4292/13/19/3926

Mihu-Pintilie, A., & Nicu, I. C. (2019). GIS-based Landform Classification of Eneolithic Archaeological Sites in the Plateau-plain Transition Zone (NE Romania): Habitation Practices vs. Flood Hazard Perception. *Remote Sensing*, *11*(8), 915. https://www.mdpi.com/2072-4292/11/8/915

Mokarram, M., & Seif, A. (2014). GIS-based automated landform classification in Zagros mountain (case study: Grain mountain). *Bulletin of Environment, Pharmacology and Life Sciences*, *3*(3), 20-32.

Ngunjiri, M. W., Libohova, Z., Owens, P. R., & Schulze, D. G. (2020). Landform pattern recognition and classification for predicting soil types of the Uasin Gishu Plateau, Kenya. *CATENA*, *188*, 104390. https://doi.org/https://doi.org/10.1016/j.catena.2019.104390

Robaina, L. E., de Souza, Trentin, R., Vargas de Cristo, S. S., & Volpato Sccoti, A. A. (2017). APPLICATION OF THE GEOMORPHONS TO THE LANDFORM CLASSIFICATION IN TOCANTINS STATE, BRAZIL *Temático de Geomorfologia (Ra'E Ga)*, *41*.

Robaina, L. E. d. S., & Trentin, R. (2020). Automated classification of landforms with GIS support. *Mercator*, *19*, e19012.

Seif, A. (2014). Landform classification by slope position classes. *Bulletin of Environment, Pharmacology Life Sciences*, *3*(11), 62-69.

Shekar, P., Raja, & Mathew, A. (2024). Morphometric analysis of watersheds: A comprehensive review of data sources, quality, and geospatial techniques. *Watershed Ecology and the Environment*, *6*, 13-25. https://doi.org/https://doi.org/10.1016/j.wsee.2023.12.001

Sissakian, V. K., & Fouad, S. F. (2015). Geological map of Iraq, scale 1: 1000 000, 2012. *Iraqi Bulletin of Geology and Mining*, *11*(1), 9-16.

Stepinski, T. F., & Jasiewicz, J. (2011). Geomorphons-a new approach to classification of landforms. *Proceedings of geomorphometry*, *2011*, 109-112.

Verhagen, P., & Drăguţ, L. (2012). Object-based landform delineation and classification from DEMs for archaeological predictive mapping. *Journal of Archaeological Science*, *39*(3), 698-703. https://doi.org/https://doi.org/10.1016/j.jas.2011.11.001

Wahyuni, D., Sukarsa, I., & Nugraha, A. S. (2021). *The Role of Geomorphological Maps in Regional Planning and Management in Indonesia (Case: Buleleng Regency, Bali)* Proceedings of the 2nd International Conference on Law, Social Sciences and Education, ICLSSE 2020, 10 November, Singaraja, Bali, Indonesia, Singaraja, Bali, Indonesia.

Yusra, A.-h. (2019). Landforms Classification of Wadi Al-Mujib Basin in Jordan, based on Topographic Position Index (TPI), and the production of a flood forecasting map. *Dirasat, Human Social Sciences*, *46*(3). https://doi.org/https://archives.ju.edu.jo/index.php/hum/article/view/15963

Zhazhlayi, P. K., & Surdashy, A. (2022). Neo-Tectonism and Quantitative Morphotectonic Analysis of Roste Valley at Imbricated-Suture Zones, Kurdistan Region, Iraq. *Iraqi Geological Journal*, *55*(2E), 35-58. https://doi.org/10.46717/igj.55.2E.3ms-2022-11-17

About the author

Dr. Kaiwan K. Fatah is a lecturer at the Salahaddin University-Erbil, College of Science, Department of Earth Sciences and Petroleum. He is a member of the Kurdistan Geologists Syndicate. He graduated from the Salahaddin University-Erbil in 2011, with a B.Sc. degree in Geology and joined the same university in 2011. He was awarded an M.Sc. degree in 2015 from the University of Southampton (the UK) in the field of Applied GIS and Remote Sensing and a Ph.D. degree in 2024 from the Salahaddin University-Erbil in the field of Applied GIS and Remote Sensing in Geo-Environmental Sciences. He has 14 years of experience working in the fields of geology, geomorphology, hydrology, geo-natural hazards, natural resources, Geo-Environmental Sciences, remote sensing, and GIS. He has 15 published articles on different geological aspects, especially in geo-natural hazards, natural resource management, Geo-Environmental Sciences, climate change, hydrology, geomorphology, land use and land cover planning, GIS, and remote sensing.

e-mail: kaiwan.fatah@su.edu.krd

Dr. Rebar T. Mzuri is a lecturer at the Salahaddin University-Erbil, College of Sciences, Dept. of Earth Sciences and Petroleum. He is a member of the Kurdistan Geological Syndicate and the Union of Iraqi Geologists. Dr. Mzuri obtained a Ph.D. in remote sensing and GIS application in Geo-environment, a master's degree in geoinformatics techniques in structural geology, and a bachelor's degree in Geology all from Salaheddin University, Erbil. He earned his post-graduate diploma in Earth Resource Exploration from the University of Twente, The Netherlands in 2009. Dr. Rebar has been researching climate change and has published numerous articles in various fields, including land degradation, vegetation analysis, flooding, drought, spatial planning, groundwater potential, air pollution, and land use planning.

e-mail: rebar.ali@su.edu.krd